Journal of the Korean Nuclear Society
Volume 27, Number 1, February 1995

Comparison of Iron(Fe) Data of ENDF/B-IV and VI in Yonggwang Nuclear Unit-3/4 Vessel Fluence Calculation

Tae Hyeong Kim and Nam Zin Cho
Korea Advanced Institute of Science and Technology
(Received August 16, 1994)

영광 3/4호기 압력용기의 중성자 조사량계산을 통한 ENDF/B-IV와 VI 철(Fe) 자료의 비교

김태형 · 조남진
한국과학기술원
(1994. 8. 16 접수)

Abstract

The accurate determination of the fast neutron flux/fluence onto the pressure vessel is an essential part of the reactor pressure vessel surveillance program. It has been reported recently that the iron cross section data in ENDF/B versions III through V might underestimate the flux/fluence of fast neutrons in steel structures such as reactor pressure vessel. In this study, for the comparison of iron data of ENDF/B-IV and VI we produced two 47-group cross section sets, CXFe-IV and CXFe-VI, which are based on Yonggwang nuclear unit-3/4 model and the iron data of ENDF/B-IV and VI, respectively. A comparison was made of the results obtained from DOT4.3 calculation using CXFe-IV and CXFe-VI. From the results, it was found that the fast flux(E > 1.0 MeV), which is important for the pressure vessel embrittlement analysis, increases by about 7.6% at the inner wall and 20% at the outer wall of the vessel, if the iron data are used from ENDF/B-VI instead of ENDF/B-IV.

요 약

원자로 압력용기에서의 정확한 속중성자 조사량의 계산은 발전소 압력용기 surveillance program의 핵심적인 부문이다. 최근 기존의 ENDF/B-III~V에 있는 철의 핵단면적 자료가 압력용기와 같은 철이 포함된 구조물에서 속중성자속을 낮게 평가하는 것으로 알려지고 있다. 본 논문에서는 ENDF/B-IV와 VI의 철(Fe) 자료의 비교를 위해 영광 3/4호기 모델과 2개의 ENDF/B 파일에 있는 각각의 철자료를 이용하여 47-에너지그룹 핵단면적집(CXFe-IV와 CXFe-VI)을 만들었다. CXFe-IV와 CXFe-VI를 사용하여 수행한 DOT4.3 계산결과에 의하면 압력용기 취화해석에 중요한 속중성자속(E > 1.0 MeV) 계산에서 ENDF/B-VI의 철자료를 사용한 경우가 ENDF/B-IV의 철자료를 사용한 경우보다 압력용기 내부표면에서 7.6%, 외부표면에서 20% 높게 나타났다.

1. Introduction

Determination of the fast neutron flux/fluence onto the pressure vessel is an essential part of the reactor pressure vessel (RPV) surveillance program. An accurate estimate of the neutron fluence is necessary to ensure the integrity of the RPV over the designed lifetime, since the embrittlement induced by irradiation may limit the life of a pressure vessel. One of the main tools for determining the pressure vessel flux is the neutron transport calculation. In transport calculation, the calculational accuracy depends partly on the cross section library used to model the composition of the reactor structures.

It has been reported recently that the iron cross section data in ENDF/B versions III through V underestimate the transmission of the fast neutrons through steel structures such as reactor pressure vessel, and this is due to the inaccuracy in the iron inelastic cross section[1~4]. In 1990, the ENDF/B-VI nuclear data file has been released by U.S. National Nuclear Data Center. The ENDF/B-VI iron data were first utilized in one-dimensional analysis for shielding problems by Williams et al.[3] and it was found the ENDF/B-VI iron data are accurate in predicting the fast neutron flux at the reactor pressure vessel. Therefore, it is of interest to examine the impact of the various iron cross section data on the vessel fluence evaluation.

In this paper, the impact of the iron data of ENDF/B-IV and VI on the RPV fluence calculation has been examined by performing the two-dimensional transport calculations. Yonggwang nuclear units 3 and 4 (YGN-3/4)[5] were chosen for the calculational model. The reactor is a Combustion-Engineering type two-loop pressurized water reactor (PWR) under construction in Korea. Table 1 shows the basic parameters of YGN-3/4. Figure 1 represents the reactor configuration showing the core, reactor structures, and surveillance capsule in quarter-core symmetry.

Table 1. The Basic Parameters of YGN-3/4

Reactor Core	
Power, MW(thermal)	2815
Height (cm)	381
Equivalent diameter (cm)	312.42
Fuel Assembly	
Assemblies in Core	177
Lattices in assembly	16×16
Pitch (cm)	20.88
Reactor Coolant	
Normal pressure (psia)	2250
Inlet temperature (°F)	564.5
Outlet temperature (°F)	621.2
Average temperature (°F)	592.9

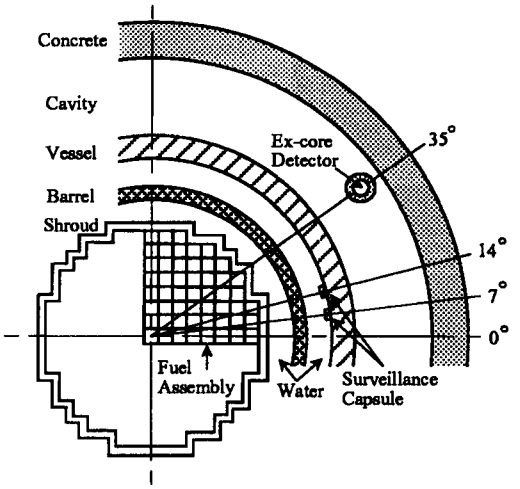

Fig. 1. Reactor Configuration of YGN-3/4

Using the YGN-3/4 model we produced two 47-group cross section sets, i.e., CXFe-IV and CXFe-VI, which are based on the iron data of ENDF/B-IV and VI, respectively. Two-dimensional calculations of the RPV fluence were then performed using DOT4.3[6] with CXFe-IV and CXFe-VI and the results compared.

2. Nuclear Cross Section Libraries

Several multigroup cross section libraries have been used for PWR pressure vessel fluence calculation and shielding problems. These libraries have different group structures and are produced via different methodologies. In this section a brief description is provided for the cross section libraries which are commonly used today.

2.1. DLC-23/CASK Library[7]

CASK has 22 neutron and 18 gamma-ray energy groups. This library was produced from ENDF/B-II neutron cross section data and DLC-12/POPLIB gamma-ray production data. Although CASK was widely used for light water reactor shielding calculations in the past few decades, it was created originally for the spent-fuel shipping cask analysis and predicts higher fast fluxes than other libraries which are based on ENDF/B-IV[1]. This library was used in YGN-3/4 design[8].

2.2. BUGLE-80 Library[9]

BUGLE-80 has 47 neutron and 20 gamma-ray energy groups and uses the P_3 Legendre approximation for the scattering angular distribution. It was created based on ENDF/B-IV and used the spectrum in the middle of the concrete wall of a PWR model for collapsing the fine-group library VITAMIN-C[10] (171 neutron groups, 36 gamma-ray groups). BUGLE-80 contains 67 nuclei and 5 materials.

2.3. SAILOR Library[11]

The energy structure of SAILOR is identical to that of BUGLE-80. This library used the space-dependent neutron spectra obtained from a one-dimensional PWR model calculation and based on VITAMIN-C. These spectra include core spectra, downcomer spectra, vessel spectra at 1/4-thickness position from the inner wall, and concrete spectra. SAILOR contains 44 nuclei and 14 materials.

2.4. ELXSIR Library[12]

ELXSIR contains 56 neutron energy groups and no gamma-ray energy groups. Above 0.1 MeV, ELXSIR has 37 energy groups, while BUGLE-80 and SAILOR have 26 groups. This library was created using the regionwise spectra which were generated from a one-dimensional transport calculation of Arkansas Nuclear One Unit 1. ELXSIR is based on ENDF/B-IV, but several materials in the library were based on ENDF/B-V. It contains 36 nuclei and 11 materials.

3. Generation of the Multigroup Cross Section Sets

3.1. Processing of the Fine-Group Cross Section Libraries

The core and structures of the reactor are modeled as the mixture of various elements. The element number densities of each material are given in Table 2. Most of data for the elements are taken from Ref. 13 while the element number densities of the RPV material are produced from Ref. 14. Since the objective of this work is to compare the impact of the iron data of ENDF/B-IV and VI on the vessel fluence calculation, we first generated two 171-group cross section sets, CXFe-IV^{171} and CXFe-VI^{171}.

CXFe-IV^{171} : For all nuclei given in Table 2, this set contains the fine-group cross section data extracted from VITAMIN-C which is based on ENDF/B-IV.

CXFe-VI^{171} : This set is identical to CXFe-IV^{171} except for the iron cross section data. In this set the 171-group iron data are generated based on ENDF/B-VI for the four isotopes (Fe^{54} ; 5.84%, Fe^{56} ; 91.68%, Fe^{57} ; 2.17%, Fe^{58} ; 0.31%), using the

NJOY91.91[15] nuclear data processing system.

3.2. ANISN Calculation and Collapsing

By a one-dimensional transport calculation, the fine-group microscopic cross sections are collapsed to obtain the multigroup macroscopic cross sections for the materials in Table 2.

The transport code ANISN[16] was used for collapsing from the fine-group library to the multigroup library. The 1-D cylindrical model of YGN-3/4 shown in Fig. 2 was used in the ANISN calculation.

ANISN calculation was performed with 132 radial meshes, P_3, and S_8 approximation. Then we created two 47-group cross section sets, CXFe-IV[47] and CXFe-VI[47](hereafter superscript 47 is omitted), by performing the 171-group eigenvalue calculation with CXFe-IV[171] and CXFe-VI[171], respectively. The 47-group energy structure is identical to that of BUGLE-80 library. For the collapsing we used the space-dependent neutron spectra from the results of ANISN calculation. Figure 3 shows the schematic procedure of generating the multigroup cross section sets.

Table 2. Element Number Densities of Materials

Material	Element	Density (b^{-1} cm^{-1})	Material	Element	Density (b^{-1} cm^{-1})
Core*	Hydrogen	2.764 −02**	Pressure	Iron	7.964 −02
	Boron	2.303 −06	Vessel	Carbon	6.514 −04
	Oxygen	2.682 −02		Manganese	1.189 −03
	Iron	6.108 −05		Nickel	7.683 −04
	Zirconium	4.518 −03		Chromium	1.947 −04
	U^{235}	1.052 −04		Molybdenum	2.782 −04
	U^{238}	6.173 −03			
	Pu^{239}	3.274 −05	Air	Nitrogen	4.340 −05
	Pu^{240}	8.981 −06		Oxygen	1.020 −05
			Ex-Core	Hydrogen	3.707 −02
Stainless	Carbon	3.169 −04	Detector	Carbon	1.211 −02
Steel	Silicon	1.694 −03	Shielding	Oxygen	1.922 −02
	Chromium	1.647 −02	Resin	Silicon	1.213 −02
	Manganese	1.732 −03			
	Iron	6.036 −02	Concrete	Hydrogen	1.487 −02
	Nickel	6.483 −03		Carbon	3.814 −03
				Oxygen	4.152 −02
				Sodium	3.040 −04
Coolant*	Hydrogen	4.688 −02		Magnesium	5.870 −04
	Boron	3.907 −06		Aluminum	7.350 −04
	Oxygen	2.344 −02		Silicon	6.037 −03
				Calcium	1.159 −02
				Iron	1.986 −04

* Based on water at temperature of 592.9 °F and pressure of 2250 psia with 500 ppm soluble boron

** Read as 2.764×10^{-2}

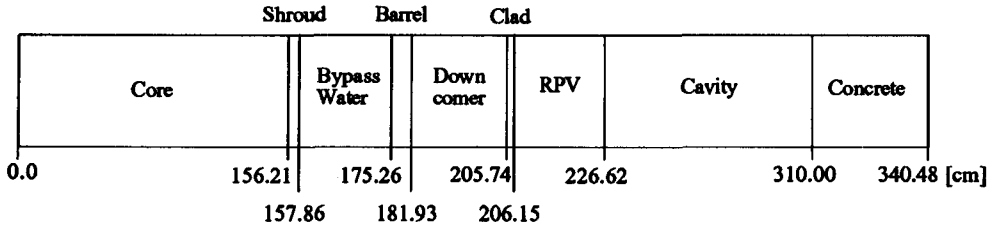

Fig. 2. YGN-3/4 One-Dimensional Model for ANISN Calculation

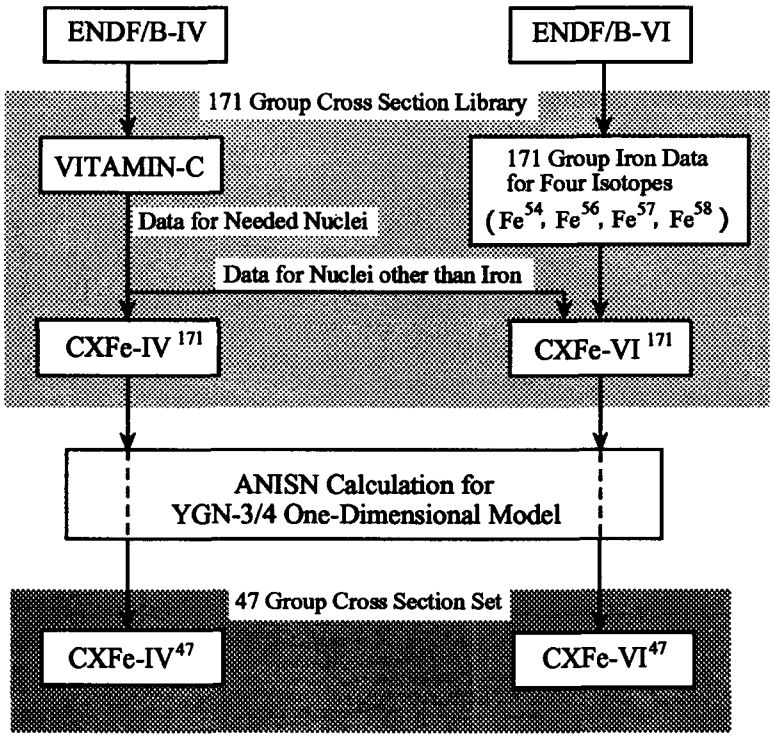

Fig. 3. Generating Procedure of Multigroup Cross Section Sets

4. Vessel Fluence Calculation

4.1. DOT 4.3 Calculation for YGN-3/4

The two-dimensional discrete ordinates transport code DOT4.3 was used in R-θ geometry to calculate the flux distributions in the structures of the reactor. Figure 4 shows the R-θ mesh distribution for one octant of YGN-3/4. A 121 radial and 92 azimuthal angle mesh structure was used. The model includes reactor core, shroud, bypass water, barrel, downcomer, surveillance capsule, RPV, cavity, ex-core detector, and concrete region.

In this study a P_3 order of scattering and an S_8

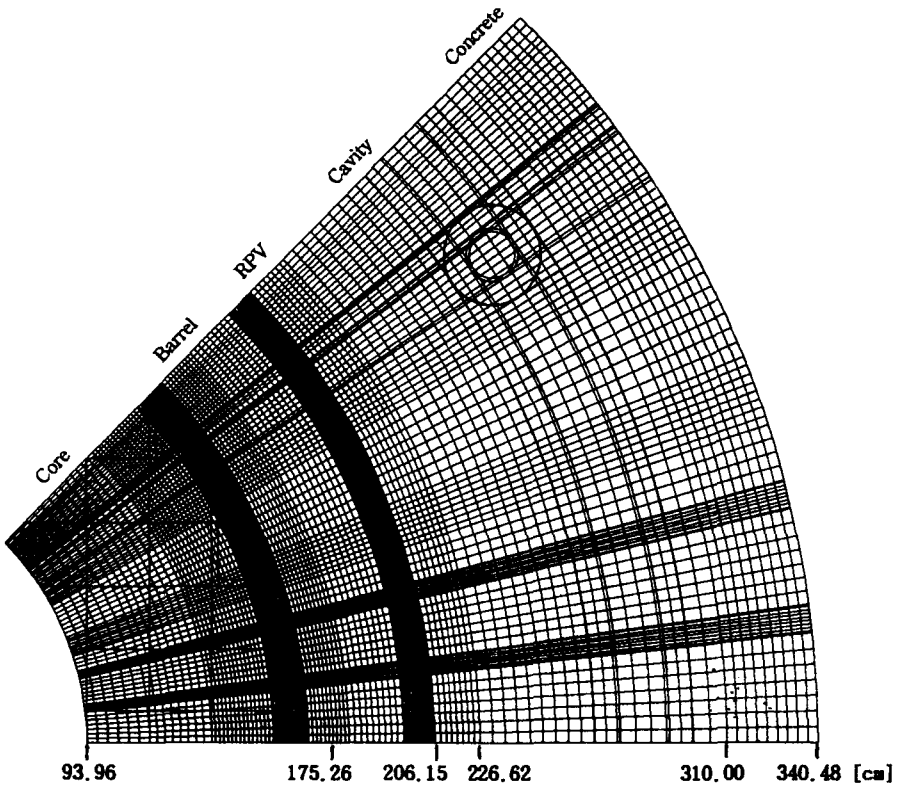

Fig. 4. *R-θ* **Model of YGN-3/4**

quadrature set were used and the flux convergence criterion for all neutron groups was 0.01%. In Fig. 4 the assemblies in core interior were replaced with the reflective boundary condition, since the neutron flux at the pressure vessel is dominated by the neutron sources in the peripheral assemblies. The neutron source distributions in the core were obtained from the system design document[8].

4.2. Results and Discussion

4.2.1. Comparison Between CXFe-IV and CXFe-VI

Figure 5 shows the fast neutron fluxes and differences along the azimuthal angle at the surveillance capsule position (R=202.48cm) obtained with CXFe-IV and CXFe-VI. In Fig. 6 the fast flux distributions at the inner wall of the RPV are shown. It is generally observed that the CXFe-VI fluxes are 7~9% higher than those calculated with CXFe-IV for both E > 1.0 MeV and E > 0.1 MeV.

Figure 7 presents the radial flux distributions for azimuthal angle 10° at which the peak flux (E > 1.0 MeV) appears at the inner wall of the vessel as shown in Fig. 6. The results show large differences outside the core, especially at the outer wall of the RPV and in the cavity where differences of ~20% are observed. This is caused by the lower value of the inelastic scattering of iron in the ENDF/B-VI data, which leads to the higher fluxes in the steel region. This phenomenon is clearly shown in Fig. 8.

Figure 8 shows the neutron spectra above 0.1 MeV

and the differences at the inner wall and the outer wall of the RPV. At the inner wall of the RPV the differences are almost ~10% for high energy regions. At the outer wall, it appears that the global behavior is similar to that seen at the inner wall of the vessel; however, the differences at the outer wall are larger than those seen at the inner wall of the

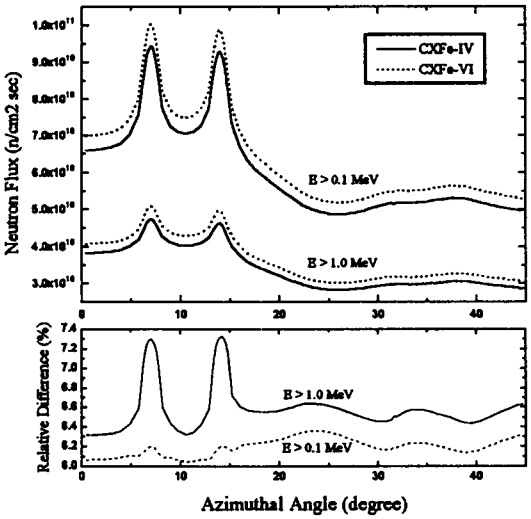

Fig. 5. Flux Distributions and Relative Difference to CXFe-IV Along the Azimuthal Angle at the Surveillance Capsule Position

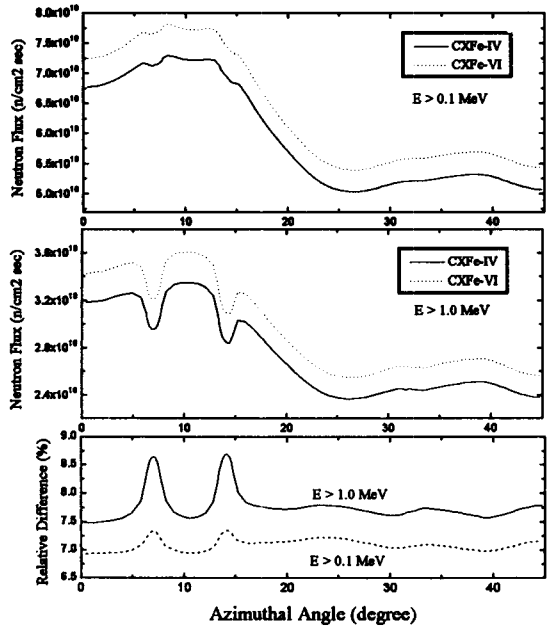

Fig. 6. Flux Distributions and Relative Difference to CXFe-IV Along the Azimuthal Angle at the Inner Wall of the RPV

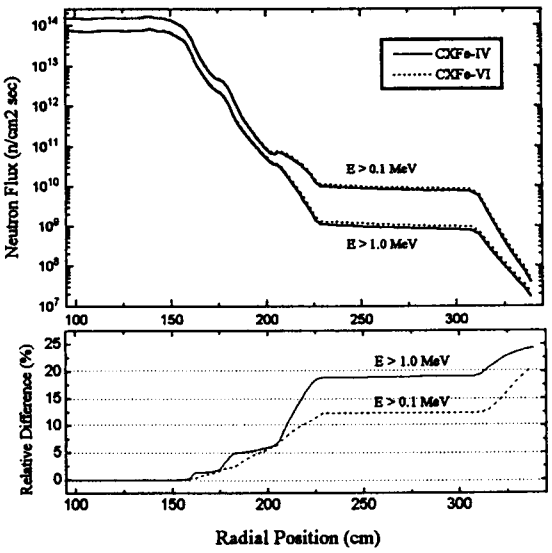

Fig. 7. Flux Distributions and Relative Difference to CXFe-IV Along the Radial Position at Azimuthal Angle 10 Degree

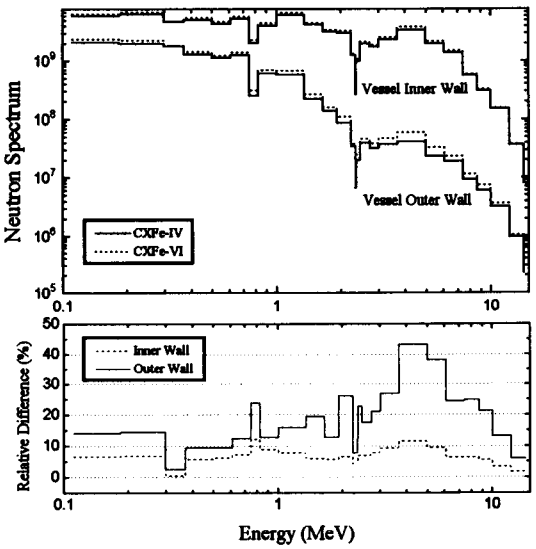

Fig. 8. Fast Neutron Spectrum and Relative Difference to CXFe-IV at the Inner Wall and the Outer Wall of the RPV

RPV. The result shows that the highest differences of ~27 to 45% occur in the energy range of 3 to 6 MeV

4.2.2. Comparison With BUGLE-80 Library

Figures 9 and 10 show comparisons of the results with the CXFe-IV, CXFe-VI, and BUGLE-80 libraries. The fast flux distributions and their comparison at the inner wall of the RPV are shown in Fig. 9. The result shows that the CXFe-IV and BUGLE-80 results are very close, while CXFe-VI predicts higher (nearly ~7%) flux than BUGLE-80. The main reason for this is because both CXFe-IV and BUGLE-80 are based on ENDF/B-IV iron data while CXFe-VI is based on ENDF/B-VI iron data.

Figure 10 shows the relative difference of the radial flux distributions at the azimuthal angle 10°. In this case the CXFe-IV data and the CXFe-VI data result in underestimation of ~30% and ~16%, respectively, compared with BUGLE-80 in the energy range above 1.0 MeV at the outer wall of the RPV and in the cavity region. Note that CXFe-IV and BUGLE-80 are based on the same cross section library. It is important to note, however, that BUGLE-80 used a PWR concrete spectrum for collapsing, while CXFe-IV and CXFe-VI used the space-dependent spectra of the YGN-3/4 one-dimensional model which is more realistic and plant-specific.

Thus, we can say that the use of the new iron data and/or space-dependent weighting functions for collapsing produces significantly different results at the outer wall of the RPV and in the cavity region.

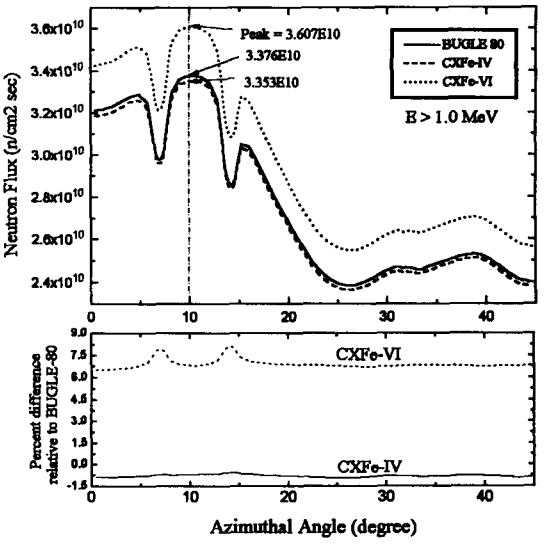

Fig. 9. Flux Distributions and Their Comparison Along the Azimuthal Angle at the Inner Wall of the RPV for CXFe-IV, CXFe-VI, and BUGLE-80

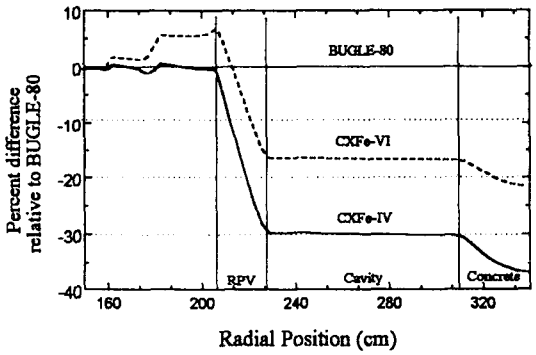

Fig. 10. Comparison of the Fast (E > 1.0 MeV) Flux Distributions Along the Radial Position at Azimuthal Angle 10 Degree for the Various Cross Section Libraries

5. Conclusions

In this study, the impact of the iron data of ENDF/B-IV and VI on the vessel fluence calculation has been examined by performing the two-dimensional transport calculations. Yonggwang nuclear units 3 and 4 were chosen as a model plant and we produced two 47-group cross section sets, CXFe-IV and CXFe-VI, which are based on the iron data of ENDF/B-IV and VI, respectively.

A comparison was made of the results obtained from DOT4.3 calculations using CXFe-IV and CXFe-VI. From the results, it was found that the flux above 1.0 MeV increases by about 7.6% at the inner

wall and 20% at the outer wall of the vessel, if the iron data are used from ENDF/B-VI instead of ENDF/B-IV. By comparison with BUGLE-80 it was also found that the use of the new iron data and/or space-dependent weighting functions for collapsing produces significantly different results at the outer regions of the pressure vessel. Thus this study confirms that the space-dependent plant-specific spectra should be used as the weighting function in collapsing the fine-group cross sections into the multigroup cross sections. The procedure of the vessel fluence calculation used in this study can be applied to other plants in a similar manner.

Acknowledgments

The authors would like to express thanks to Jung Do Kim of Korea Atomic Energy Research Institute (KAERI) for helping us in processing the ENDF/B-VI iron data to perform this study. They also wish to thank Hyeong Heon Kim of KAERI for his helpful comments on the YGN-3/4 model. This study was supported in part by the Ministry of Science and Technology of Korea.

References

1. A. Haghighat and R. Veerasingam, "Transport Analysis of Several Cross-Section Libraries Used for Reactor Pressure Vessel Fluence Calculations," *Nucl. Tech.*, **101**, 237 (1993)
2. H.S. Basha and M.P. Manahan, "A Comparison of the BUGLE-80, SAILOR, and ELXSIR Neutron Cross-Section Libraries for PWR Pressure Vessel Surveillance Dosimetry and Shielding Applications," *Nucl. Tech.*, **100**, 79 (1992)
3. M.L. Williams et al., "Transport Calculations of Neutron Transmission Through Steel Using ENDF/B-V, Revised ENDF/B-V and ENDF/B-VI Iron Evaluations," *Ann. Nucl. Energy*, **18**, 549 (1991)
4. 김정도, 길충섭, "철의 개량된 평가핵자료를 이용한 가압경수로 압력용기의 중성자 투과 계산," 94 춘계학술발표회 논문집, Vol. 1, pp. 93, 한국원자력학회 (1994)
5. "Yonggwang Nuclear Units 3 and 4, Preliminary Safety Analysis Report," Korea Electric Power Corporation (1988)
6. W.A. Rhoades and R.L. Childs, "An Updated Version of the DOT4 One- and Two-Dimensional Neutron/Photon Transport Code," *ORNL-5851*, Oak Ridge National Laboratory (1982)
7. R.W. Roussin, "CASK-81, 22 Neutron, 18 Gamma-Ray Group, P_3 Cross Section for Shipping Cask Analysis", *DLC-23*, ORNL (June 1981)
8. H.H. Kim, "YGN-3/4 Vessel Fluence Evaluation," *10487-NRE-055*, KAERI (1992)
9. R.W. Roussin, "BUGLE-80, Coupled 47 Neutron, 20 Gamma Ray, P_3 Cross Section Library for Light Water Reactors," RSIC-DLC-75, ORNL (June 1980)
10. R.W. Roussin et al., "VITAMIN-C: The CTR Processed Multigroup Cross Section Library for Neutronics Studies," *ORNL-RSIC-37* (July 1980)
11. G.L. Simmons and R. Roussin, "SAILOR, Coupled, Self-shielded, 47 Neutron, 20 Gamma-ray, P_3, Cross Section Library for Light Water Reactors," *RSIC-DLC-76* (1985)
12. M.L. Williams et al., "The ELXSIR Cross Section Library for LWR Pressure Vessel Irradiation Studies: Part of the LEPRICON Computer Code System," *EPRI NP-3654* (September 1984)
13. J.G. Ahn, N.Z. Cho and J.E. Kuh, "Generation of Spatial Weighting Functions for Ex-Core Detectors by Adjoint Transport Calculation," *Nucl. Tech.*, **103**, 114 (1993)
14. D.H. Song et al., "Fatigue and Fracture Properties of Korean-Making Reactor Vessel Steel," *Proceedings of the International Symposium on Pressure Vessel Technology and Nuclear Codes & Standards*, Seoul, Korea, pp. 13-43 to 13-50 (April 1989)
15. R.E. Macfarlane et al., "The NJOY Nuclear Data Processing System, Volume I: User's Manual," *LA-9303-M*, Vol. I (ENDF-324) (May 1982)

16. W.W. Engle, Jr., "ANISN-ORNL : A One-Dimensional Discrete Ordinates Transport Code with Anisotropic Scattering," *CCC-254* (October 1975)